Journal of Alloys and Compounds 617 (2014) 455–463

Contents lists available at ScienceDirect

Journal of Alloys and Compounds

journal homepage: www.elsevier.com/locate/jalcom

Effect of thermal treatment on the interfacial reaction, microstructural and mechanical properties of Zn–Al–SnO_2/TiO_2 functional coating alloys

O.S.I. Fayomi [a,b,*], A.P.I. Popoola [a], V.S. Aigbodion [c]

[a] Department of Chemical, Metallurgical and Materials Engineering, Tshwane University of Technology, P.M.B. X680, Pretoria, South Africa
[b] Department of Mechanical Engineering, Covenant University, P.M.B 1023, Ota, Ogun State, Nigeria
[c] Department of Metallurgical and Materials Engineering, University of Nigeria, Nsukka, Nigeria

ARTICLE INFO

Article history:
Received 2 May 2014
Received in revised form 7 July 2014
Accepted 20 July 2014
Available online 7 August 2014

Keywords:
Composite-reinforcement
Chemical interaction
Microstructures
Co-deposition
Thermal treatment
Wear

ABSTRACT

In this paper, the microstructure and thermal treatment behavior of Zn–Al–SnO_2/TiO_2(Zn–Al–Sn/Ti) produced through co-deposition route was investigated. 7.0–13.0 wt% TiO_2 and SnO_2 was added to Zn–Al bath. Thermal treatment was done for 2 h at 200 °C, 400 °C and 600 °C. The ageing characteristics of the coated alloys were evaluated using (SEM/EDS) and XRD. The hardness and wear value of the thin film were examined with micro-hardness and UMT-2 sliding tester respectively. The corrosion properties were evaluated by linear polarization in 3.65% NaCl. From the result obtained, the coating exhibited good stability. The uniform distribution of the composites on the fabricated alloy and age-treatment were the major factor responsible for the mechanical and electrochemical improvement. The optimum value was obtained at Zn–Al–7Sn–Ti–0.3V–S for as-coated and Zn–Al–7Sn–Ti–0.3V–S at 400 °C for the thermal-aged samples. The stabilities in hardness and corrosion resistance against the working substrate were attributed to the formation of coherent and uniform precipitation in the metal lattice.

1. Introduction

The massive impact of zinc based coatings for steel protection before the emergence of new materials for engineering enhancement is enormous. They exhibit good electro-oxidation resistance in ambient atmospheric medium but their life-span decrease in a more aggressive environment due to corrosion product initiation and wear fracture [1–6]. Effort to improve on this limitation has been tremendously attested for from literature by various authors on the use of composite coatings [7–16]. The primary intention on the choice of composite particulate was due to their significant constituent of solid grains and matrix metal [1,17,18].

Lately researcher have step ahead to understand the process and preparation of this composite materials, the mechanism behind the enhanced particle and the re-crystallization tendency [18–36]. Reinforced metal matrix composite electro-deposition like TiO_2 [25,27,28], SiO_2 [18,30], ZrO_2 [20], Cr_2O_3 [17,29], Al_2O_3 and ZnO [22,25,35] has proven to provide crucial characteristics. Meanwhile for excellent application especially in high temperature performance, high surface modifications are required and incorporation of high temperature composite particle had been attested to give such protection [9–11,37]. Unfortunately, binary composite fabrications through electro-deposition are prone to possess possible limitation for high temperature application, wear and corrosion environment.

Although, report affirmed that the control of process parameter has been major consideration in metal matrix composite co-deposition. The wear, corrosion resistance, thermo-mechanical stability and tribo-oxidation behavior of binary alloy composite coating have been reported to give more stability at low temperature applications [24,31–34]. Few works have been done on ternary and quaternary alloy composite coating of Al_2O_3, TiO_2 and SnO_2 especially when subjected to the heat-treatment and wear behavior for multifunctional application [23,25,32]. There is no doubt that excellent composite coating properties are highly dependent on the stable dispersion of the nanoparticles in plating bath; corrosion resistance can be affected by the microstructure, crystal grain, texture and above all the additive particle. Much recent attention has been focused on the development of techniques for electroplating alloys such as zinc–iron, zinc–nickel, and zinc–cobalt. The operating parameters and applications of these coatings are very similar to those for unalloyed zinc. There were many efforts by researchers worldwide to developed zinc alloy coating and zinc–metallic/non-metallic composites coating that will enhance better properties than ordinary zinc coating.

In view of the tribological and poor thermal stability of the binary composite coating, our focus in this work is to provide a

* Corresponding author. Tel.: +27719811277
E-mail address: ojosundayfayomi3@gmail.com (O.S.I. Fayomi).

http://dx.doi.org/10.1016/j.jallcom.2014.07.141
0925-8388/

modified growth interface and morphology by quaternary fabricated metal oxide composite coating, which will offer excellent thermo-mechanical stability, better corrosion properties and tribo-oxidation mechanism. The tribological properties of surface coated particles were evaluated using sliding wear machine and their morphological crystal structure/topography was characterized by means (SEM/EDS and OPM). The phase studies were examined with the help of X-ray diffractometer (XRD).

2. Experimental procedure

2.1. Preparation of substrates

Rectangular sectioned flat specimens of commercially sourced mild steel of (40 mm × 20 mm × 1 mm) sheet was used as cathode substrate and 99.5% zinc plate of (30 mm × 20 mm × 1 mm) were prepared as anodes. The initial surface preparation was performed with finer grade of emery paper as described in our previous studies [35]. The sample were properly cleaned with sodium carbonate, pickled and activated with 10% HCl at ambient temperature for 10 s then followed by instant rinsing in deionized water. The mild steel specimens were obtained from metal sample site Nigeria. The chemical composition of the sectioned samples was shown in Table 1 as obtained from spectrometer analyzer.

Table 1
Chemical composition of mild steel used (wt%).

Element	C	Mn	Si	P	S	Al	Ni	Fe
Composition	0.15	0.45	0.18	0.01	0.031	0.005	0.008	Balance

2.2. Processed composition

The electrolytic chemical bath of Zn–Al–Sn–Ti fabricated alloy was performed in a single cell containing two zinc anode and single cathode electrodes as described schematically in Fig. 1 and Table 2. The distance between the anode and the cathode was 15 mm. Before the plating, all chemical used are analar grade and de-ionized water were used in all solution admixed. The bath was preheated at 40°C. The processed parameter and bath composition admixed used for the different coating matrix is as follows Zn 75 g/L, Al 30 g/L, K_2SO_4 50 g/L, $ZnSO_4$ 75 g/L, Boric acid 10 g/L, $SnO_2$7 g-13 g/L, TiO_2 7 g–13 g/L, pH 4.8, time, 20 min and tempt 40 °C. The choice of the deposition parameter is in line with the preliminary study from our previous work [23,35].

The prepared zinc electrode were connected to the rectifier at varying applied potential and current density between 0.3 V and 0.5 V at 2 A for 20 min. The distance between the anode and the cathode with the immersion depth were kept constant as described by Subramanian et al. [34,35]. The fabricated were rinsed in distilled water and samples air-dried. Portion of the coating were sectioned for characterization.

2.3. Characterization of coating

The structural evolution of the deposited composite coating alloy was characterized with VEGA TESCAN Scanning electron microscope equipped with EDS. The phase change was verified with XRD. Micro-hardness studies were carried out using a Diamond pyramid indenter EMCO Test Dura-scan micro-hardness testers at a load of 10 g for a period of 20 s. The average microhardness trend was measured across the coating interface at interval of 2 cm using screw gauge attached to the Dura hardness tester.

2.4. Friction and wear tests

The friction and wear properties of the deposited quaternary fabricated alloy were measured using CERT UMT-2 tribological tester at ambient temperature of 25 °C with schematic diagram as shown in Fig. 2. The reciprocating sliding tests

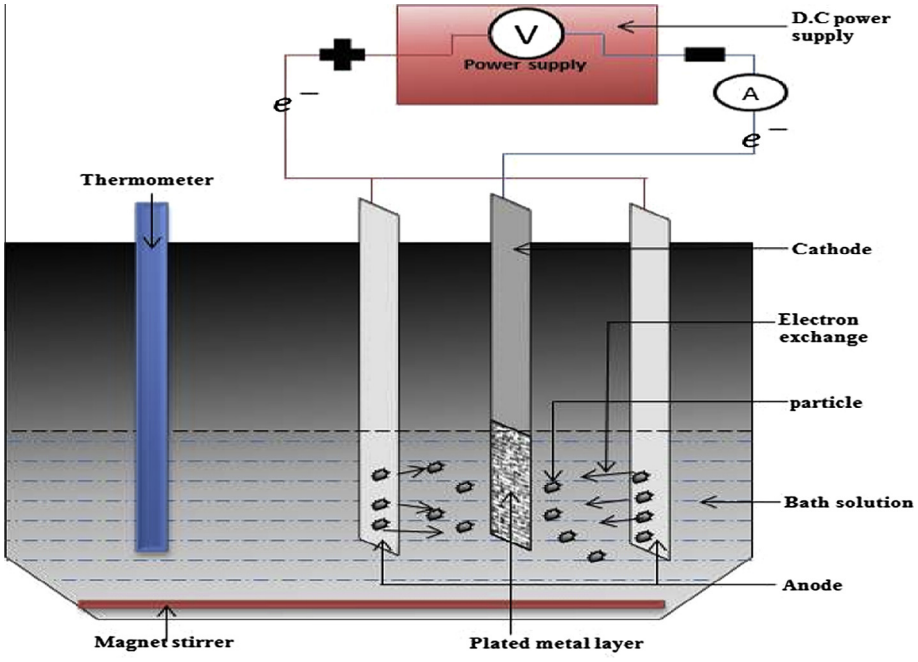

Fig. 1. Schematic diagram of electrodeposited system.

Table 2
Itinerary bath composition of quaternary Zn–Al–Sn–Ti–Salloy co-deposition.

Sample order	Material sample	Time of deposition (min)	Potential (V)	Current (A)	Con. of additive (g)
Blank	–	–	–	–	–
Sample 1	Zn–Al–7Sn–Ti–0.3V–S	20	0.3	2	7
Sample 2	Zn–Al–7Sn–Ti–0.5V–S	20	0.5	2	7
Sample 3	Zn–Al–13Sn–Ti–0.3V–S	20	0.3	2	13
Sample 4	Zn–Al–13Sn–Ti–0.5V–S	20	0.5	2	13

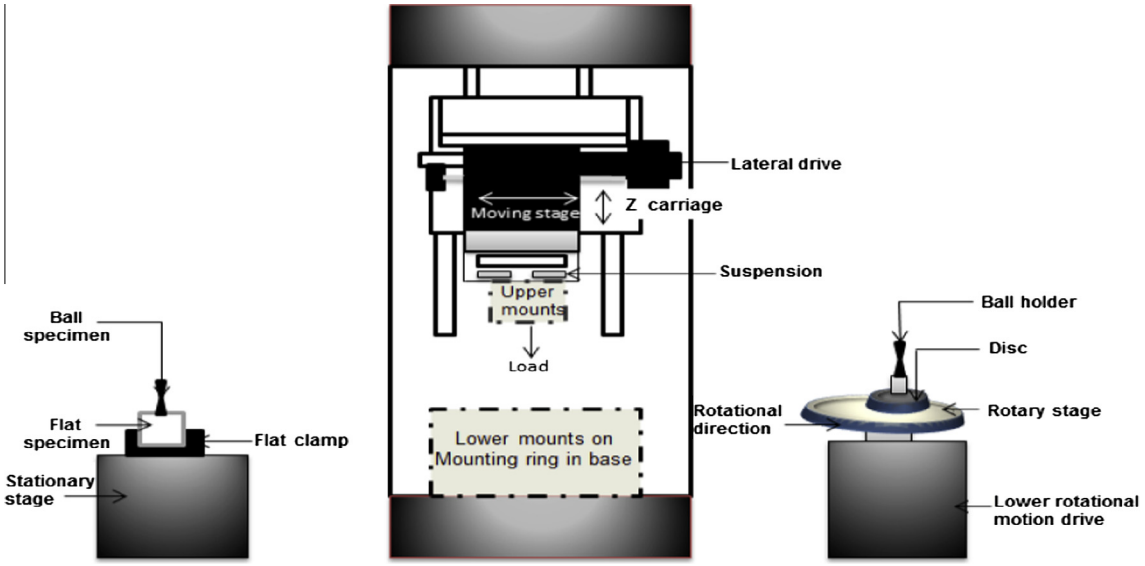

Fig. 2. Schematic view of reciprocating sliding friction CERT UMT-2 test system.

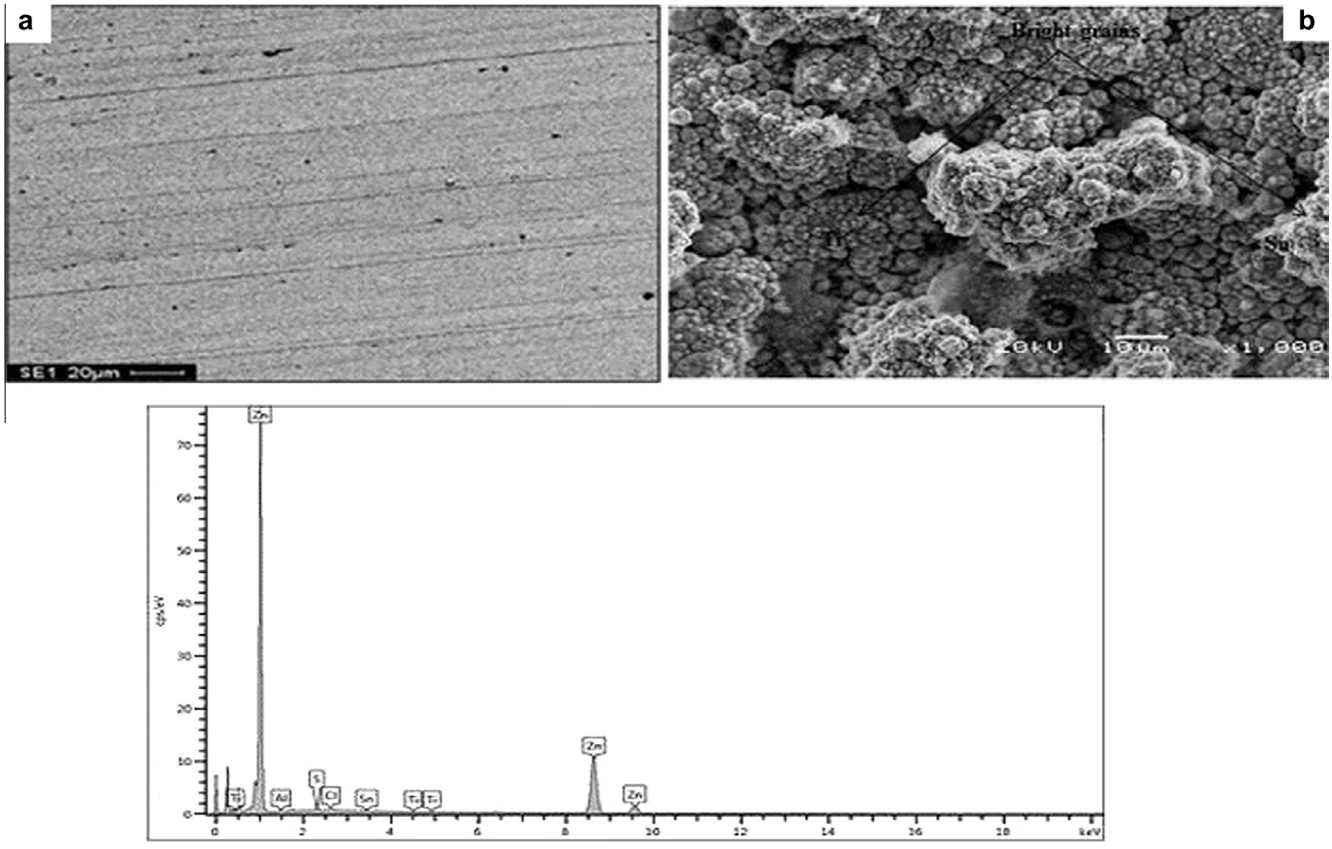

Fig. 3. Micrograph showing the surface morphology of (a) SEM of mild steel substrate (b) SEM/EDX of Zn–Al–7Sn–Ti–0.3V sulphates composite coating.

was carried out with a load of 5 N, constant speed of 5 mm/s, displacement amplitude of 2 mm in 20 min. A Si_3N_4 ball (4 mm in diameter, HV50g1600) was chosen as counter body for the evaluation of tribological behavior of the coated sample. The dimension of the wear specimen was 2 cm by 1.5 cm as prescribed by the specimen holder. After the wear test, the structure of the wear scar and film worn tracks were examined with the help of high nikon optical microscope (OPM) and scanning electron microscope couple with energy dispersive spectroscopy (VEGAS-TESCAN SEM/EDS).

2.5. Thermo/electro-oxidation test

Isothermal heat treatment (Direct fired furnace atmosphere) of Zn–Al–Sn–Ti composite coating was carried out between 200 and 600 °C for 1 h to enhance the mechanical stability of the coated samples. The electrochemical studies were performed with Autolab PGSTAT 101 Metrohmpotentiostat using a three-electrode cell assembly in a 3.65% NaCl static solution at 40 °C. The developed composite was used as the working electrode, platinum electrode was used as counter electrode

and Ag/AgCl was used as reference electrode. The anodic and cathodic polarization curves were recorded by a constant scan rate of 0.012 V/s which was fixed from ±1.5 mV. From the Tafel corrosion analysis, the corrosion rate, potential and linear polarization resistance was obtained.

3. Results and discussion

3.1. Structural evolution studies

SEM micrograph trace of the substrate and the deposited alloy was presented in Fig. 3. The coating exhibits good morphology with adorable structural grain and smaller particulate within the interface. The presence of the dispersed metal composite could be seen from Fig. 3b showing different grain size with good texture and phases. EDS also confirm the presence of the individual element. A visible coverage by composite micro-crystallites without crack was seen. The structure yield good quality of deposit which was attributed to the miscible and good control of process parameter of the bath as reported by Praveen and Venkatesha [2,34,35]. Additionally, the compact and bright crystal might also be link to the influence of additive admixed in the bath thereby preventing the initiation of stress propagation [22,25]. Composite conditioning from their individual behavior might result to excellent coating stability and mass loss reduction. Hence the lower crystal growth and nucleation within the interface alter the progression of the Sn, Ti and Al additive conditioned.

3.2. XRD studies

Fig. 4 shows the XRD patterns of the produced Zn–Al–7Sn–Ti–S–0.3Vdeposited composite coating. From the pattern, visible phases were seen with generation of intermetallic growth like Zn, ZnSn, $ZnAl_2Sn$, Zn_2Al_3Ti, ZnTi were presence. The presence of the intermediate dispatched composite phases observed was traceable to their inter-diffusion mechanism and ion of each particulate as described by Hu and Wang [37]. In the other hand, vivid progressions of Zn hexagonal structure from all peak diffraction line were seen [28,36,37]. Hence the phase modification and new orientation of the metal matrix are indication of the harness performance and remarkable effect of the composite induced. Although, the result expected is not far from desire expectation reason been that, two critical assumptions were foreseen from unset. Firstly, it is believe that zinc ions could maximally affect the crystal size and growth in co-deposited matrix and this would generate and improved the existence of the dispatched particle. Secondly the co-deposition mechanism could be easily altered for effective preferred matrix orientation as a result of a conditioned composite metal. This results was in line with the studies made by Fustes et al. [28].

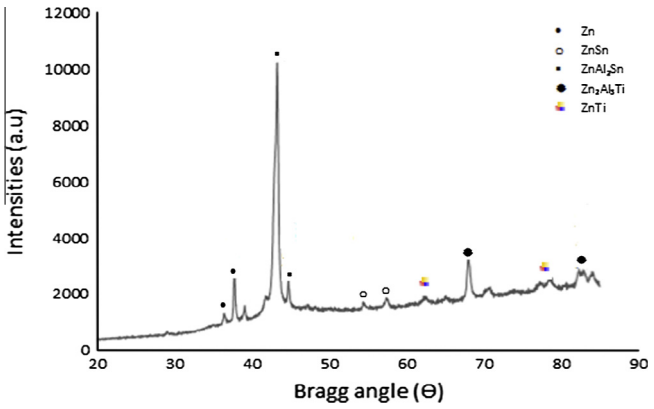

Fig. 4. X-ray diffraction pattern for Zn–Al–7Sn–Ti–0.3V.

3.3. Wear rate evaluation

Fig. 5 shows the plot and the summarized wear loss of the variation in line with sample deposition respectively. The wear rate was very high for the as-received sample compared to all Zn–Al–Sn–Ti–S matrixes at various process parameters. From the composite deposited coating, Zn–Al–7Sn–Ti–S–0.3V possesses a lower wear loss difference in all with 0.001 N reason for this improvement might be due to better stability as a results of good movement of particle size distribution and uniformity at the interface as seen from the structural studies. More so, it is essential to mention that the potential of composite additive might have form

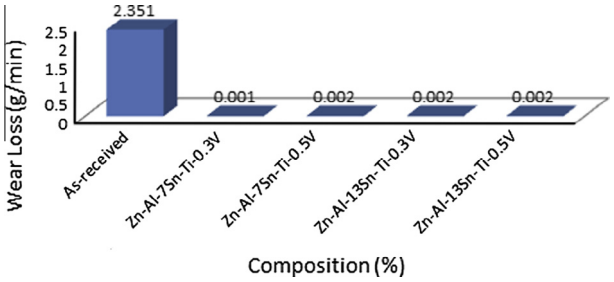

Fig. 5. Variation of the wear loss with time of Zn–Al–Sn–Ti.

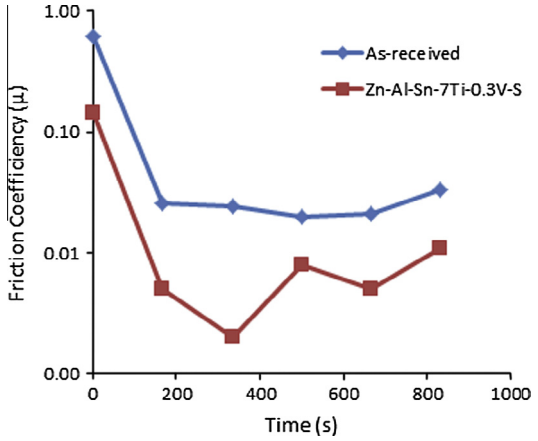

Fig. 6. Variation of wear friction co-efficient against time for Zn–Al–7Sn–Ti–0.3V sulphates deposited sample.

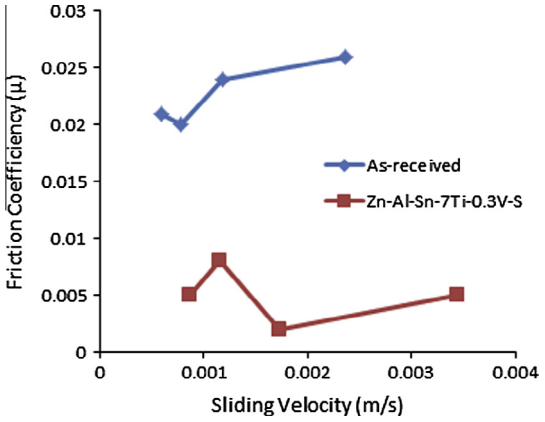

Fig. 7. Variation of wear friction co-efficient against sliding velocity for Zn–Al–7Sn–Ti–0.3V sulphates deposited sample.

a stable layer which provides such anti-wear activities seen from all composite induced coatings.

In the other hand, the mechanism behind this retard dislocation within the composite co-deposited layers might also be traced to the multiphase structure of the alloy consisting of major anti-rich composite particulate of aluminium–tin–titanium within the zinc-rich phases. Other admix matrix had 0.002 of weight loss. Ordinarily, individual characteristics of this metal composite could positively influence the wear loss trend much more at their intermediate state. Reports by Wang et al. [18,35] unveiled that the adhesion of a film to substrate is synonymy to wear rate properties; from their studies, the wear off of deposited coating is a function of poor adhesion and mechanical stability of the fabricated coatings. At this point, it is noteworthy to say that the phenomena of wear stability is attributed to the massive contribution of the metal matrix composite, their individual solid grain and the process parameter that provide the stable films layer [1,36].

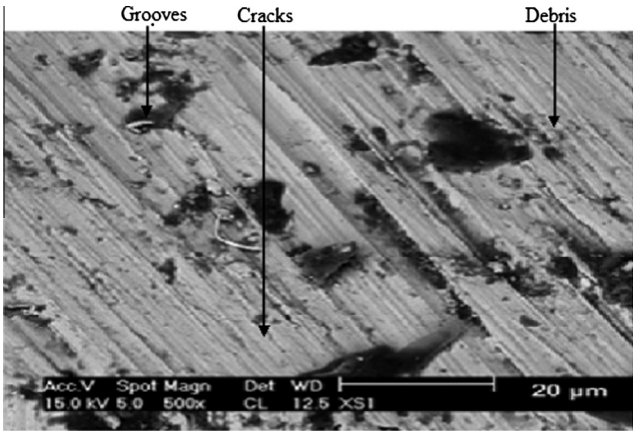

Fig. 8. SEM images of the wear scar of mild steel.

The wear characteristics of best coating among the variance is Zn–Al–7Sn–Ti–S–0.3V which was compare with the as-received in term of co-efficient of friction against the time as shown in Fig. 6. The obtained composite induced coatings films provide lower co-efficient of friction as the trend of coating goes on the interface over time of wear. The wear life of the deposited coating have a consistence behavior downward till 200 s beyond it, the wear friction coefficient become irregular but still maintained a good performance against the substrate.

The sinusoidal trend observed might be due to the un-homogeneous nature of the crystal at the interface due to the particle induced and the in consistence of the throwing power from the process. In all, a decrease in the plane track of coefficient of friction is an indication of the enhanced improvement of the co-deposited alloy with about 0.048 differences. For further critical observation of the typical profile in Fig. 6, the coefficient of friction of the as-received sample quickly attained a steady trend from 200 s to 800 s which is due to the accelerated deterioration of the as-received sample seen than when compared with the co-deposited alloy that fluctuated before reaching the time stipulated. This behavior suggested that the coatings could have reduces the wear

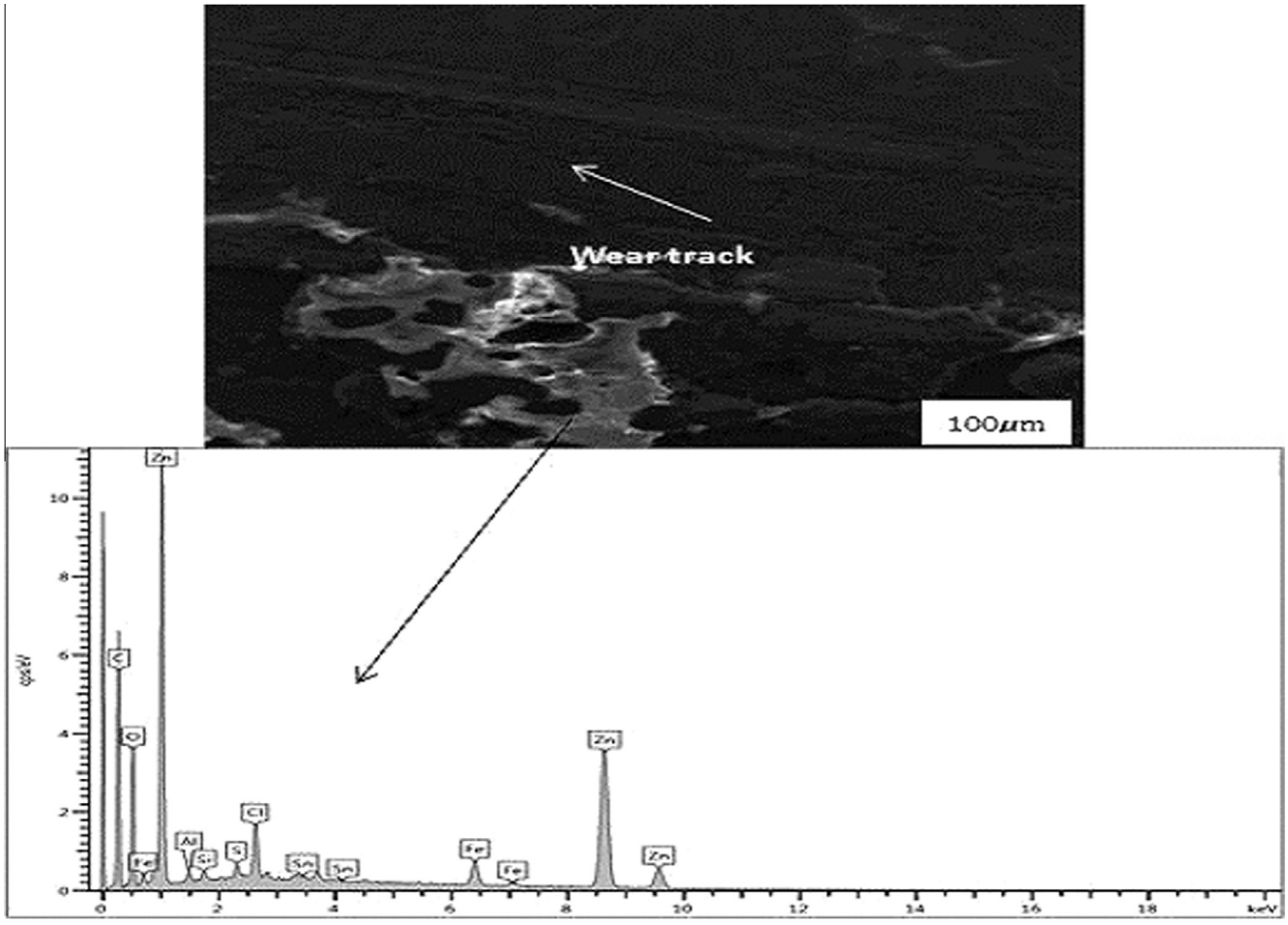

Fig. 9. SEM/EDS images of the wear scar of deposited alloy.

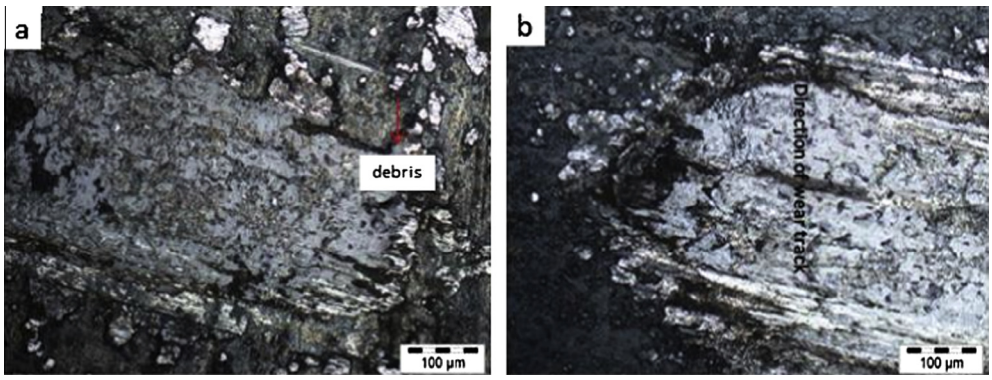

Fig. 10. OPM Micrograph of the wear scar for (a) Zn–Al–7Sn–Ti and (b) Zn–Al–13Sn–Ti sulphates deposited sample.

rate influence as affirmed in the previous studies by Mo et al. [33,35,36]. Fig. 7, likewise gives the details friction coefficient traces against sliding velocity. The wear properties were also considered between the coated and the based sample with over 100% improvement in all. The life span of the as-received mild steel substrate was lower as the coefficient of friction rises geometrically. It is also observed that the stability of the coated film alloy were function of the new counter-body formed which systematically influence and reduce the wear to frictional occurrences [35,38].

Figs. 8 and 9 show the microscopic examination of worn surfaces of the based substrate and the coated sample of Zn–Al–7Sn–Ti–S–0.3V quaternary alloy. From the scar, larger degree of plastic deformation, massive grooves, pits and fracture can be seen on the surface of the as received sample as shown in Fig. 8. The impact of the reciprocating sliding disc was high on the substrate as the penetration lead to visual stress and fracture. With the coated sample Zn–Al–7Sn–Ti–S–0.3V a better appearance were seen.

Definitely the embedded conditioned composite matrix could have been responsible for this wear resistance especially with the presence of Al, TiO_2 and SnO_2. Although authors have adoringly guided that metal oxide have been used in bath to project oxide barrier coating but [21] reported in his preliminary literature of composite studies that mixed oxide formed can provide excellent wear resistance properties. In view of this, unseen plastic deformation from coated alloy is a strong indication of the early report that the formation of oxide films on the wear surfaces of these alloys provides a higher wear resistance as expected with other feasible composition and elemental phases still seen from ED's spectra.

It should be noted that stable adhesion has a better flow than the visible irregular degradation of the later. Comparison of the composite coatings at different applied voltage and additive concentration were also found necessary to be examined through OPM studies as shown in Fig. 10. From the alloy coating Fig. 10a with Zn–Al–7Sn–Ti–S–0.3V matrix still gave a better wear scar though few cracks were found beside the wear track region. More so, the continues increase in coefficient of friction during wear mechanism could increase severe plastic deformation [38,39] which is in with our finding where large dry cavity was seen along the direction of Zn–Al–13Sn–Ti–0.3V sample.

In general, no serious fracture or excessive stress found on both coating morphologies, the accumulation of debris were minimal and the presence of the composite induced were obviously still seen in both coating along the wear track direction. At this point, the tribo-oxidation stability of the quaternary alloy has proven to be excellent and a typical inference could be easily made about the stable nature of the inter-composite induced behavior for improved wear resistance as a result of the compactable adhesive strength of the fabricated coating under a prescribe process parameter.

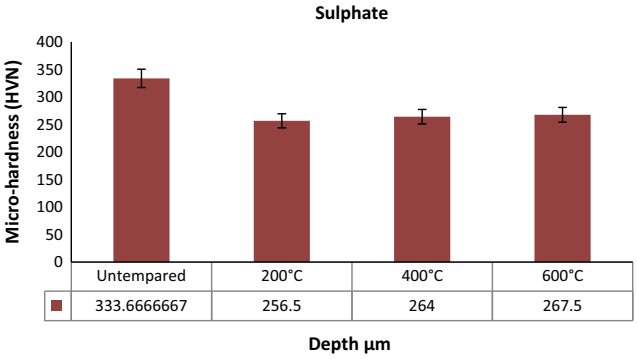

Fig. 11. Micro-hardness variation of coated and heat treated matrix.

3.4. Thermal stability/photo-recrystallization studies

Fig. 11 shows the hardness properties of the deposited quaternary coating before and after heat treatment and the process parameter used to evaluate their thermal-oxidation characteristics are presented in Table 3. The subjected thermally induced alloy at 200 °C, 400 °C and 600 °C were observed to have possessed beyond expectation good stability against thermal shock at 2 h. The subjected coating at 600 °C has build-up scale which could strengthen hardenability. In general, there is quite little reduction in hardness properties compare to the coated samples without heat-treatment. Mechanical behavior due to the thermal treatment and porosity within the alloy surface could result in hardness propagation. Few literatures also attested that the compression stress could significantly improve the micro-hardness when it is much less than the ultimate strength of the coating but [17] reported that the defect such as porosity, macro-particle at the alloy surface will have detrimental effect on the mechanical properties. At this point, the slight pile up at higher temperature of 600 °C could still maintain better recrystallization stability of the coatings but if treated above twice the subjected thermal shock process can lead to unexpected deterioration.

Obviously the ceramics/composite metal oxide phases likely formed might be responsible and necessitate the good hardened and resistance to any excessive external forces. Hence, further addition of the particles in the Zn–Al matrix might improve its thermal stability by acting as a barrier to dislocation motion and hence reducing the grain growth if bath parameters are well controlled [1,19].

Fig. 12a and b shows the SEM/EDS image of the photo-structural morphologies of the Zn–Al–7Sn–Ti–S–0.3V after heat-treatment in 400 °C and 600 °C for 2 h to affirm their interfacial structural change. Since our interest is tailored on high temperature 200 °C

Table 3
Itinerary heat-treatment system of the quaternary co-deposition alloy.

Sample order	Material sample	Time of deposition (min)	(Temp. °C)	Heat-treated, *T* (h)
Sample 1	Zn–Al–7Sn–Ti–0.3V–S	20	Nil	2
Sample 2	Zn–Al–7Sn–Ti–0.3V–S at 200 °C	20	200	2
Sample 3	Zn–Al–7Sn–Ti–0.3V–S at 400 °C	20	400	2
Sample 4	Zn–Al–7Sn–Ti–0.3V–S at 600 °C	20	600	2
				2

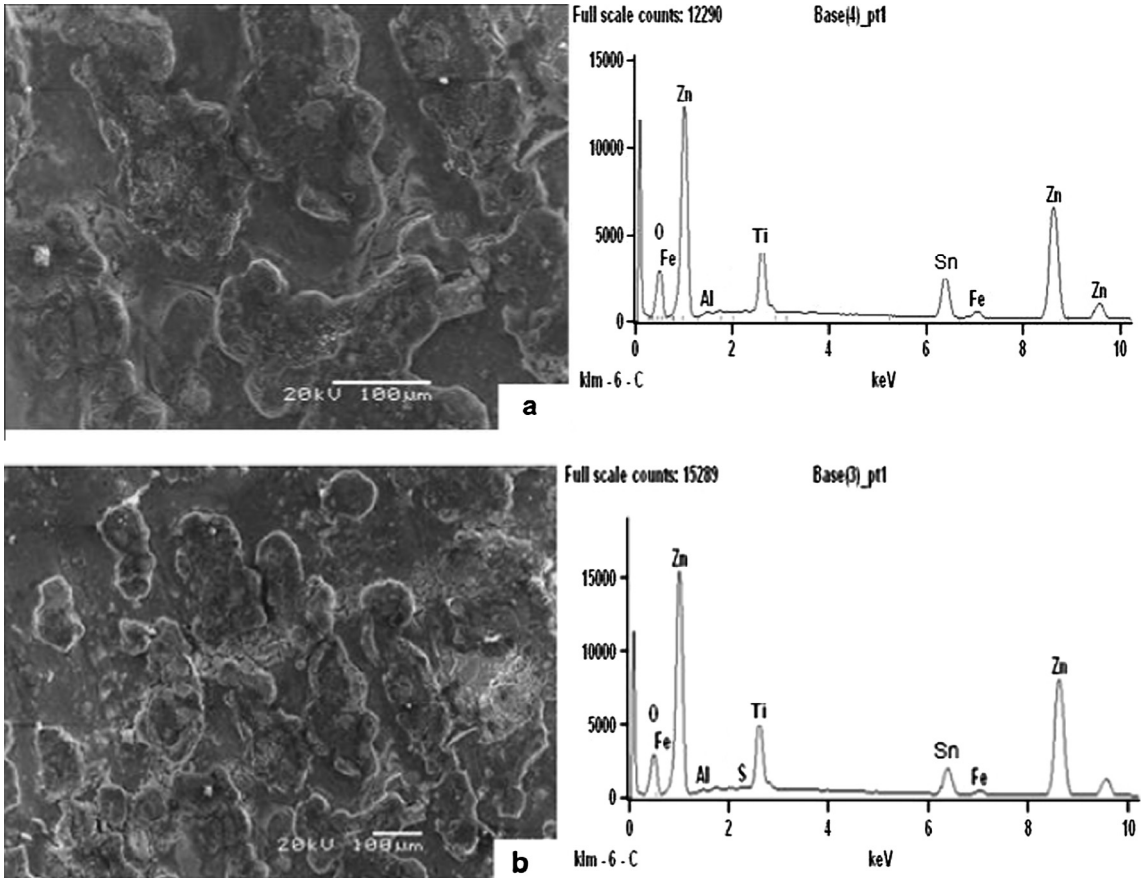

Fig. 12. SEM/EDS morphologies of heat-treated sample of Zn–Al–7Sn–Ti–S–0.3V of (a) 400 °C and (b) 600 °C.

might not necessary be affected. Beyond 200 °C it was seen that the recrystallization took place and a new phase modified orientation was observed. Although the EDS spectra still confirm the presence of the admixed composite metal within the surface regardless of the change in the crystal. In the other hand, structure and growth through the help of the additive are still seen which is in line with report by Gomes et al. [22] that solid materials for interesting application are obtained from micron and sub-micron particle. [5,12]. Also mention that grain size and porosity of the coating has larger effect on the morphology and the corrosion propagation. Hence, the deformation resistances here in the study are traceable to the bonding force that the composite ceramics oxide produced into the lattice of the zinc-rich system over the cathode.

The linear electro-thermal oxidation polarization resistance of Zn–Al–7Sn–Ti–S–0.3V matrix at 200 °C, 400 °C and 600 °C behavior was described in Fig. 13. The summarized polarization data were described in Table 4. The oxidation resistances were however favored the composites alloy coating without heat-treatment; an indication of significant correlation with the hardness stability phenomena. We could see that the passive layer of the heat-treated zone/fabricated alloy reduces as the temperature goes

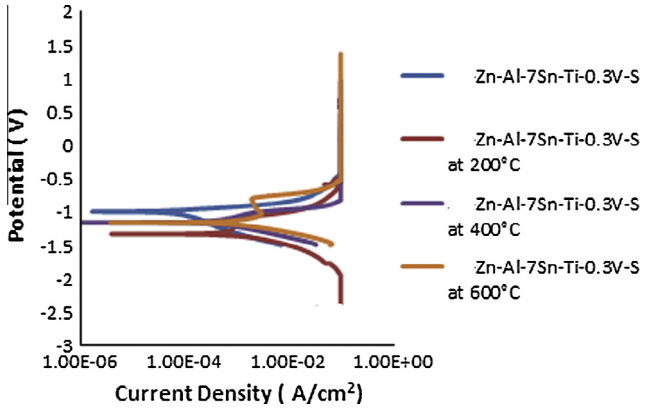

Fig. 13. Electrochemical polarization results of tempered Zn–Al–Sn–Ti in sulphates bath.

beyond 400°C due to slight pill up of scale at grain boundary. Although our expectation is to see recrystallization, deformation and severe corrosion rate occurring because of the two simultaneous

Table 4
Summary of the potentiodynamic polarization results of heat-treated and unheated Zn–Al–Sn–Ti in sulphates bath at varies temperature.

Sample No.	I_{corr} (A/cm^2)	R_P (Ω)	E_{corr} (V)	Corrosion rate (mm/yr)
As-received	7.04E-02	27.600	-1.539000	4.100000
Z n - A l -7 S n - Ti -0.3 V- S	8.58**E** - 07	1718.6	-0.999451	0.001856
Z n - A l - 7 S n - Ti - 0.3V -S at 200 °C	0.000162	51.771	-1.3351	1.885800
Z n - A l-7 S n - Ti - 0.3V -S at 400 °C	8.22**E** - 05	76.169	-1.163300	0.955370
Z n - A l -7 S n - Ti - 0.3V -S at 600 °C	0.000141	57.774	-1.165000	1.640600

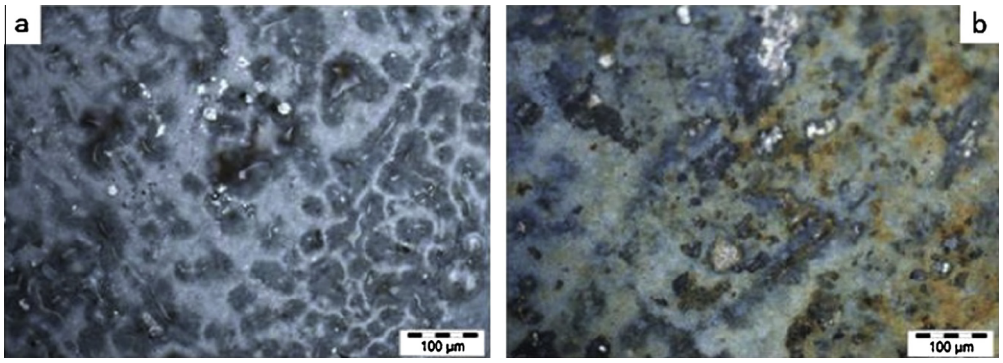

Fig. 14. Optical micrograph of the heat-treated Zn–Al–7Sn–Ti sulphates deposited sample after corrosion of (a) 400 °C and (b) 600 °C.

stress induced system (Thermal and Chemical Oxidation Process). However, the adhesion behavior of the alloy film was strong enough to resist to some extend the deterioration instead more oxide formation in white nature were seen.

It is heartfelt to see a successful improvement of coating even after thermal–chemical resistance of coated sample against the as-received substrate. The corrosion potential of the least corrosion observed heat-treated alloy is about −1.3351 mv. This effect possesses doubled geometric improvement over the as-received sample at −1.539 mv. The corrosion rate and current density of the entire coated sample decreased significantly down as temperature induced decreases. Although, anticorrosion resistance properties of any composite are always seen toward modify morphology and good adhesion properties [22,35,36]. The polarization resistance of the entire coated sample improved in the following trend 1 > 3 > 4 > 2 with the Rp values of 1.718.6 Ω, 76.169 Ω, 57.774 Ω, and 51.771 Ω. The corrosion rate value also followed the same trend with 0.001856 mm/y, 0.95537 mm/y, 1.6406 mm/y and 1.8858 mm/y respectively.

The OPM images of heat-treated Zn–Al–7Sn–Ti–S–0.3V after exposure to corrosion were presented in Fig. 14a and b. The result revealed dispatch oxide layer within the entire morphology even after severe stress. New orientation and structure were seen from Fig. 14a with 400 °C sample. However, at 600 °C little exposure of the embedded composite was found at the interface which might be an indication of the chloride and oxide scales which is known as corrosion product.

4. Conclusions

From the results and discussion above the following conclusions can be made:

1. Uniform and adherent quaternary Zn–Al–Sn–Ti alloy composite coating was successfully deposited on mild steel substrate with a simple sulphates bath through a well control process parameter.
2. Good uniform growth, perfect crystal and bright metal matrix composite deposit was obtained. The electrochemical corrosion resistance increase geometrical against the as-received sample.
3. The incorporation and conditioning of the metal composite in this study greatly improved the thermal stability, microhardness, wear trend and corrosion resistance of the fabricated quaternary sulphates coating. In addition, the increase in corrosion resistance of Zn–Al–7Sn–Ti–S–0.3V is not only as results of substantial Ti/Sn alloy phase but formation of Zn/Al deposits which provide good surface orientation.
4. Zn–Al–Sn–Ti coatings with difference additive% show significant differences in tribological properties thus showing limited wear and low friction coefficient.
5. New crystalline structures are formed as a result of heat-treatment with Zn–Al–7Sn–Ti–S–0.3V coating, thereby possessing best properties among all series. Thermal stability of the composite coating improved with the addition of Sn and Ti. Good morphology significantly distorts easy penetration of the temperature within the coating interface.

Acknowledgements

This material is based upon work supported financially by the National Research Foundation. The equipment support by Surface Engineering Research Centre (SERC) Tshwane University of Technology, Pretoria is deeply appreciated.

References

[1] V. Kanagalasara, V.V. Thimmappa, Appl. Surf. Sci. 257 (2011) 8929.
[2] B.M. Praveen, T.V. Venkatesha, Appl. Surf. Sci. 254 (2008) 2418.
[3] R.E. Melchers, R. Jeffrey, Corros. Sci. 47 (2005) 1678.
[4] L. Chuen-Chang, H. Chi-Ming, J. Coat. Technol. Res. 3 (2006) 99.
[5] O.S.I. Fayomi, A.P.I. Popool, Int. J. Electrochem. Sci. 8 (2013) 11502.
[6] R.E. Melchers, B.B. Chernov, J. Corros. Sci. 52 (2010) 449.
[7] R.E. Melchers, J. Corros. Sci. 49 (2007) 3149.
[8] A.P.I. Popoola, O.S. Fayomi, Sci. Res. Essay 6 (2011) 4264.
[9] C. Mohankumar, K. Praveen, V. Venkatesha, K. Vathsala, O. Nayana, J. Coat. Technol. Res. 9 (2012) 71.
[10] A.P.I. Popoola, O.S. Fayomi, Int. J. Electrochem. Sci. 6 (2011) 3254.
[11] M.M. Abou-Krisha, F.H. Assaf, S.A. El-Naby, J. Res. Coat. Technol. 6 (2009) 391.
[12] M.J. Rahman, S.R. Sen, M. Moniruzzaman, K.M. Shorowordi, J. Mech. Eng. 40 (2009) 9.
[13] M. Arici, H. Nazir, A. Aksu, J. Alloys. Comp. 509 (2011) 1534.
[14] R. Xu, J. Wang, Z. Guo, H. Wang, J. Rare Earth 26 (2008) 579.

[15] G. Yang, S. Chai, X. Xiong, S. Zhang, L. Yu, P. Zhang, Trans. Nonferr. Met. Soc. China 22 (2012) 366.
[16] O. Sancakoglu, O. Culha, M. Toparli, B. Agaday, E. Celik, J. Mater. Des. 32 (2011) 4054.
[17] C.T. Kwok, F.T. Cheng, H.C. Man, J. Surf. Coat. Technol. 200 (2006) 3544.
[18] T.G. Wang, D. Jeong, Y. Liu, S. Lyengar, S. Melin, K.H. Kim, J. Surf. Coat. Technol. 206 (2012) 2638.
[19] O. Hammami, L. Dhouibi, P. Bercot, E.M. Rezrazi, E. Triki, Int. J. Corros. Sci. 8 (2012) 1.
[20] X. Zhu, C. Cai, G. Zheng, Z. Zhang, J. Li, Trans. Nonferr. Met. Soc. China 21 (2011) 2216.
[21] S.M.A. Shibli, F. Chacko, C. Divya, J. Corros. Sci. 52 (2010) 518.
[22] A. Gomes, T. Frade, I.D. Nogueira, Curr. Microsc. Contrib. Adv. Sci. Technol. 2 (2012) 1146.
[23] O.S.I. Fayomi, M. Abdulwahab, A.P.I. Popoola, J. Ovonic Res. 9 (2013) 123.
[24] T. Frade, Z. Bouzon, A. Gomes, M.I. Da Silva, M.I. Pereira, Surf. Coat. Technol. 204 (2010) 3592.
[25] W. Zhang, W. Liu, C. Wang, J. Eur. Ceram. Soc. 22 (2002) 2869.
[26] A. Abdel, M.A. Barakat, R.M. Mohamed, Appl. Surf. 254 (2008) 4577.
[27] A.A. Abdel, H.B. Hassan, Abdel, M.A. Rahim, J. Electroanal. Chem. 620 (2008) 17.
[28] J. Fustes, A.D.A. Gomes, M.I. Silva Pereira, J. Solid State Electrochem. 121 (2008) 1435.
[29] M. Srivastava, J.N. Balaraju, B. Ravishankar, K.S. Rajam, Surf. Coat. Technol. 205 (2010) 66.
[30] D. Dong, X.H. Chen, W.T. Xiao, G.B. Yang, P.Y. Zhang, Appl. Surf. Sci. 255 (2009) 7051.
[31] A.P.I. Popoola, O.S.I. Fayomi, O.M. Popoola, Int. J. Electrochem. Sci. 7 (2012) 4898.
[32] H. Kazimierezak, P. Ozga, Surf. Sci. 607 (2013) 33.
[33] J.L. Mo, M.H. Zhu, B. Lei, Y.X. Leng, N. Huang, Deposition Phys. Vap. Deposition Wear 263 (2007) 1423.
[34] B. Subramanian, S. Mohan, S. Jayakrishnan, Surf. Coat. Technol. 201 (2006) 1145.
[35] O.S.I. Fayomi, A.P.I. Popoola, Res. Chem. Intermed. Res. 39 (2013) N06, http://dx.doi.org/10.1007/s11164-013-1354-2. ISSN 0922-6168.
[36] A.P.I. Popoola, O.S.I. Fayomi, O.M. Popoola, Int. J. Electrochem. Sci. 7 (2012) 4860.
[37] C. Hu, C. Wang, Electrochim. Acta 51 (2006) 4125.
[38] Y. L Su, W.H. Kao, Tribol. Int. 36 (2003) 11.
[39] B. Bhushan, G.S. Theunissen, X. Li, Thin Solid Films 311 (1997) 67.